Journal of
PERIODONTAL RESEARCH

J Periodont Res 2017; 52: 761–771

JOURNAL OF PERIODONTAL RESEARCH
doi:10.1111/jre.12446

Effects of glucose concentration on osteogenic differentiation of type II diabetes mellitus rat bone marrow-derived mesenchymal stromal cells on a nano-scale modified titanium

I. Yamawaki[1], Y. Taguchi[1], S. Komasa[2], A. Tanaka[3], M. Umeda[1]

[1]Department of Periodontology, Osaka Dental University, Osaka, Japan, [2]Department of Removable Prosthodontics and Occlusion, Osaka Dental University, Osaka, Japan and [3]Department of Oral Pathology, Osaka Dental University, Osaka, Japan

Yamawaki I, Taguchi Y, Komasa S, Tanaka A, Umeda M. Effects of glucose concentration on osteogenic differentiation of type II diabetes mellitus rat bone marrow-derived mesenchymal stromal cells on a nano-scale modified titanium. J Periodont Res 2017; 52: 761–771. © 2017 John Wiley & Sons A/S. Published by John Wiley & Sons Ltd

Background and Objective: Diabetes mellitus (DM) is a common disease worldwide. Patients with DM have an increased risk of losing their teeth compared with other individuals. Dental implants are a standard of care for treating partial or full edentulism, and various implant surface treatments have recently been developed to increase dental implant stability. However, some studies have reported that DM reduces osseointegration and the success rate of dental implants. The purpose of this study was to determine the effects of high glucose levels for hard tissue formation on a nano-scale modified titanium surface.

Material and Methods: Titanium disks were heated at 600°C for 1 h after treatment with or without 10 M NaOH solution. All disks were incubated with type II DM rat bone marrow-derived mesenchymal stromal cells before exposure to one of four concentrations of glucose (5.5, 8.0, 12.0 or 24.0 mM). The effect of different glucose concentrations on bone marrow-derived mesenchymal stromal cell osteogenesis and inflammatory cytokines on the nano-scale modified titanium surface was evaluated.

Results: Alkaline phosphatase activity decreased with increasing glucose concentration. In contrast, osteocalcin production and calcium deposition were significantly decreased at 8.0 mM glucose, but increased with glucose concentrations over 8.0 mM. Differences in calcium/phosphate ratio associated with the various glucose concentrations were similar to osteocalcin production and calcium deposition. Inflammatory cytokines were expressed at high glucose concentrations, but the nano-scale modified titanium surface inhibited the effect of high glucose concentrations.

Yoichiro Taguchi, DDS, PhD, Department of Periodontology, Osaka Dental University, 8-1 Kuzuhahanazonocho, Hirakata, Osaka 573-1121, Japan
Tel: +81-72-864-3084
Fax: +81-72-864-3184
e-mail: taguchi@cc.osaka-dent.ac.jp

Key words: bone marrow cells; hyperglycemia; osseointegration; titanium dioxide

Accepted for publication December 9, 2016

Conclusion: High glucose concentration increased hard tissue formation, but the quality of the mineralized tissue decreased. Furthermore, the nano-scale modified titanium surface increased mineralized tissue formation and anti-inflammation, but the quality of hard tissue was dependent on glucose concentration.

Diabetes mellitus (DM) is a common metabolic disorder characterized by hyperglycemia due to impaired insulin secretion, insufficient insulin activity, or both (1). The main types of DM include type I and type II. Type I DM is associated with pancreatic β-cell destruction and accounts for 5–10% of subjects with diabetes. Type II DM is associated with a relative, rather than an absolute, insulin deficiency and accounts for 90–95% of all individuals with DM (2). Chronic hyperglycemia has been associated with tissue damage because endothelial cells take up glucose passively in an insulin-independent manner (3).

It is well known that DM is associated with the development of periodontitis, which can cause loss of teeth (4). Dental implant prosthesis has become an effective treatment approach in recent years. However, DM has been considered a relative contraindication for implant treatment because of increased susceptibility to infection, delayed wound healing and microvascular complications (5). In general, later studies suggest that patients with DM tend to have a lower success rate of implant osseointegration than otherwise healthy patients because DM exposes the patient to incomplete and delayed bone healing around implant fixtures with immature and less organized newly formed bone (6–12). Many researchers have developed various processed implants to prevent periimplantitis (13–20). Because of this competition, there has been substantial improvement in the physical structure of the surface, with increased surface roughness promoting an improved bone response (21–26).

We have previously reported that a nano-network structure on a titanium surface, induced by alkali etching, markedly enhanced cell adhesion, proliferation and osteogenesis. These effects were most pronounced when the concentration of NaOH was 10 M, indicating the great potential of this alkali in improving the clinical performance of bone implants (27). By changing the properties of the oxide layer, different tissue responses can be induced. A simple oxide modification method is heat treatment, which induces the formation of a thick oxide layer; this has a beneficial effect on the tissue response.

Khandelwal *et al.* (28) demonstrated a predictable, clinically successful implant prosthesis, even in patients with DM who lack good glycemic control. This supported the application of the dental implant prosthesis for patients with a broader range of glycemic control than was traditionally proposed. Moreover, McCracken *et al.* (29) reported increased bone volume around dental implant fixtures in diabetic rats compared with insulin-treated and control rats, but the bone tissue quality was not as well organized.

The regulation of insulin levels in DM is related to bone marrow-derived mesenchymal stromal cells (BM-MSCs) (30–32). Our previous study investigated the effects of a titanium surface with nano-network structures on osteogenic differentiation in BM-MSCs (33). We aimed to investigate the effects of glucose concentration on osteogenic differentiation on a nano-scale modified titanium surface using bone marrow stromal cells.

The purpose of this study was to clarify the effects of different glucose concentrations on osteogenic differentiation and extracellular matrix (ECM) mineralization of type II DM rat BM-MSCs on a nano-scale modified titanium surface *in vitro*.

Material and methods

Disk preparation

Titanium disks (15 mm in diameter) were punched out from sheets of 1 mm thick grade 2 pure titanium (Daido Steel, Osaka, Japan). These disks were classified into two groups: the oxide (Ox) group was heated at 600°C for 1 h using a dental laboratory full auto ring furnace (SRF-650; Morita Inc., Kyoto, Japan); and the nano-sheet oxide (NSx) group was immersed in 10 M NaOH solution, and placed for 24 h in an oil bath maintained at 30°C (27). The solution in each flask was replaced and treated with distilled water, and this procedure was repeated until the solution reached a conductivity of 5 μs/cm. The disks were dried at room temperature and then heated at 600°C for 1 h.

Surface characterization

The titanium surface topography was qualitatively evaluated using a scanning electron microscope (S-4000; Hitachi High-Technologies Co., Tokyo, Japan) and an atomic force microscope (SPM-9600; Shimadzu Co., Tokyo, Japan). Contact angles were measured using a video contact angle measurement system (VSA 2500 XE; AST Products, Tokyo, Japan) at room temperature, in 3 μL of ultrapure water.

The constituent elements of the titanium surface were measured using wide range X-ray photoelectron spectroscopy (PHI X-tool; ULVAC-PHI Inc., Kanagawa, Japan). Measurement conditions were as follows: X-ray source, Al Kα; X-ray condition,

15 kV 4 W; analytical range, 24 μm; take-off angle, 45°; neutralizing gun conditions, 1.2 eV and 20.0 μA.

Cell culture

BM-MSCs were isolated from the femurs of 8 wk old Goto–Kakizaki (GK) rats, a model for type II DM. This study was performed under the Guidelines for Animal Experimentation of Osaka Dental University (approval no. 1508001). Briefly, rats were killed using 4% isoflurane (Pfizer Inc., New York, NY, USA), and the bones were aseptically excised from the hind limbs. The proximal end of the femur and the distal end of the tibia were clipped. A 21-gauge needle (TERUMO, Tokyo, Japan) was inserted into the hole in the knee joint of each bone, and the marrow was flushed from the shaft with growth medium containing Eagle's minimal essential medium (Nacalai Tesque Inc., Kyoto, Japan) supplemented with 10% fetal bovine serum (FBS; Fraction V; Pierce Biotechnology, Rockford, IL, USA), penicillin (500 U/mL; Nacalai Tesque), streptomycin (500 μg/mL; Nacalai Tesque) and fungizone (1.25 μg/mL; Nacalai Tesque). The resulting marrow pellet was dispersed by trituration, and the cell suspensions from all bones were combined in a centrifuge tube.

Passage 3 cells were seeded at a density of 4×10^4 cells/cm^2 into 24-well tissue culture plates (Becton Dickinson Labware, Franklin Lakes, NJ, USA) containing titanium disks. The cells were cultured at 37°C in a humidified 5% CO_2/95% air atmosphere.

Measurement of cell proliferation

Cell proliferation was measured using the CellTiter-Blue Cell Viability Assay (Promega, Madison, WI, USA) according to the manufacturer's protocol. Briefly, BM-MSCs were seeded on the samples at a density of 4×10^4 cells/cm^2. After culturing BM-MSCs on the disks for 2 d, the medium was removed and replaced with medium containing 10% FBS, penicillin (500 U/mL; Nacalai Tesque), streptomycin (500 μg/mL; Nacalai Tesque), fungizone (1.25 μg/mL; Nacalai Tesque) and glucose (5.5, 8.0, 12.0 or 24.0 mM), and allowed to attach for 3, 6 and 72 h. At each prescribed time point, non-adherent cells were removed by rinsing with phosphate-buffered saline (PBS). CellTiter-Blue Reagent (50 μL) and PBS (250 μL) were then added to each well. After incubation at 37°C for 1 h, the solution was removed from the 24-well tissue culture plates (Becton Dickinson Labware) and 100 μL was added to a new 96-well tissue culture plate (Becton Dickinson Labware). The OD560/590 of the remaining solution was measured. The difference between the two optical densities was defined as the proliferation value.

Cell differentiation in various glucose concentrations

After culturing BM-MSCs on the disks for 7 d, the medium was removed and replaced with osteogenic differentiation medium containing 10% FBS and osteogenic supplements: 10 mM β-glycerophosphate (Nacalai Tesque), 80 mg/mL of ascorbic acid (Nacalai Tesque), 10 nM dexamethasone (Nacalai Tesque) and glucose (four concentrations). The glucose concentrations for this study were chosen to reflect normal, postprandial and high glucose values, similar to those seen in DM. In brief, the normal glucose concentration of 5.5 mM is equivalent to 99 mg/dL, while the postprandial concentration of 8.0 mM corresponds to 144 mg/mL, and the high glucose concentrations of 12.0 and 24.0 mM are approximately equal to 216 and 432 mg/dL, respectively. Differentiation medium were replaced every 2 d.

Alkaline phosphatase activity

After 1 wk of osteogenic culture, cells were washed with PBS lysed with 200 μL of 0.2% Triton X-100 (Sigma-Aldrich, St. Louis, MO, USA) and the cell lysates were transferred to a microcentrifuge tube containing a 5 mm hardened steel ball. Tubes were agitated on a shaker (Mixer Mill Type MM 301; Retsch Gmbh & Co., Haan, Germany) at 29 Hz for 20 s to homogenize the sample. Alkaline phosphatase (ALP) activity was measured using the Alkaline Phosphatase Luminometric ELISA Kit (Sigma-Aldrich) according to the manufacturer's protocol. The reaction was terminated with 3 N NaOH to a final concentration of 0.5 N NaOH, and p-nitrophenol production was measured by determining the absorbance at 405 nm using a 96-well microplate reader (SpectraMax M5; Molecular Devices, Sunnyvale, CA, USA). DNA contents were measured using the DNA Assay Kit (PicoGreen dsDNA Assay Kit; Invitrogen, Carlsbad, CA, USA) according to the manufacturer's protocol. To normalize ALP activity, ALP levels were normalized to the amount of DNA in the cell lysates.

Osteocalcin analysis

The sandwich enzyme immunoassay used in this study was specific for rat osteocalcin and can measure its levels directly in the culture supernatant after 4 wk of osteogenic culture. Osteocalcin levels in cell culture supernatants were measured according to the manufacturer's instructions (Rat Osteocalcin ELISA Kit DS; DS Pharma Biomedical Co., Ltd., Osaka, Japan).

Extracellular matrix mineralization

ECM mineralization by BM-MSCs was evaluated by Alizarin Red staining (Sigma-Aldrich). After 4 wk of osteogenic culture, the cells were stained with Alizarin Red for 10 min at room temperature. Cell monolayers were washed with distilled water until color was absent and images were acquired.

Calcium (Ca) deposited in the ECM was measured after dissolution with 10% formic acid. Ca levels were quantified using a Ca test kit (Calcium E-test Kit; Wako, Osaka, Japan). After 4 wk of osteogenic culture, 1 mL Calcium E-Test chromogenic reagent and 2 mL buffer solution were added to 50 μL of collected medium, and the absorbance of the reaction products was measured at 610 nm

using a 96-well microplate reader (Molecular Devices). Ca ion concentrations were calculated from the absorbance values relative to a standard curve.

Phosphate (P) deposition in the ECM was measured after dissolution with 10% formic acid. Levels of P were quantified using a P test kit (Malachite Green Phosphate Assay Kits; BioAssay Systems, Hayward, CA, USA). Working reagent (20 μL) was added to each 80 μL of the acid reagent, and the absorbance of the reaction product was measured at 600–660 nm using a 96-well microplate reader (Molecular Devices). Each P ion concentration was calculated from the absorbance value relative to a standard curve.

Gene expression

Gene expression was evaluated using a real-time reverse-transcription polymerase chain reaction (PCR) assay (TaqMan®; Applied Biosystems, Thermo Fisher Scientific, Waltham, MA, USA). GK rat BM-MSCs were seeded on to Ox and NSx disks at a density of 4×10^4 cells/cm^2 in normal culture medium (1 mL/well). After 7 d culture to enable cell adherence, the medium was replaced with osteogenic differentiation medium containing glucose (5.5, 8.0, 12.0 or 24.0 mM) and cells were cultured for a further 3 or 4 wk. Total RNA was isolated using a kit (RNeasy Mini Kit; Qiagen, Venlo, the Netherlands). RNA (10 μL) from each sample was reverse transcribed into complementary DNA using a kit (PrimeScript® Reagent Kit; Takara Bio, Otsu, Shiga, Japan). Gene expression for tumor necrosis factor-alpha (TNF-α), interleukin (IL)-1β and IL-6 (Taqman® Gene Expression Assay; TNF-α; Rn01525859_g1, IL-1β; Rn00580432_m1, IL-6; Rn01410 330_m1) was quantified using PCR (StepOnePlus Real-Time PCR System; Applied Biosystems, Thermo Fisher Scientific). The reactive gene expression rate for each group was calculated using the ΔΔCt method, assuming the gene expression rate of the negative control group.

Statistical analysis

Data were analyzed using SPSS 19.0 software (SPSS IBM, Armonk, NY, USA). All experiments were performed in triplicate. All data are shown as the means ± standard deviation (SD). In all analyses, statistical significance was determined using one-way analysis of variance (ANOVA) followed by a Fisher's least significant difference test. Values of $p < 0.05$ were considered significant.

Results

Titanium surface analysis

Scanning electron microscopy surface analysis identified fine scratches in the Ox group and a fine intricate network structure in the NSx group (Fig. 1A). Three-dimensional atomic force microscopy surface imaging in the phase mode showed a smooth surface on the Ox group and a fine network structure of nanometer scale on the NSx group (Fig. 1B).

Cross-sectional views identified water droplets on the surface of the disks in the Ox and NSx group, and their contact angles were depicted. A marked difference in contact angles was found between the Ox and NSx groups. The NSx group had increased significantly wettability compared with the Ox group (Fig. 1C).

The constituent elements of each titanium surface were measured by X-ray photoelectron spectroscopy to determine the degree of surface pollution and oxidation. The surface of the NSx disks had more oxygen elements than the Ox disks. Furthermore, the Ox and NSx disks had no carbon elements, regardless of nano-scale processing (Fig. 1D).

Cell proliferation

Cell proliferation on the disks after 3, 6 and 72 h of culture was assessed (Fig. 2). The difference between Ox and NSx was measured at all culture times. High glucose concentration promoted cell proliferation on the Ox disks, but did not promote cell proliferation on the NSx disks after 6 and 72 h of culture.

Production of osteogenic-related proteins

ALP activities were determined in the Ox and NSx groups at the four concentrations of glucose in osteogenic medium at 1 wk of culture. ALP activity decreased significantly depending on the glucose concentration in both the Ox and NSx groups. Additionally, ALP activity in the NSx group was higher compared with the Ox group at all glucose concentrations (Fig. 3A).

Osteocalcin production was also determined on the surface of both groups at the four concentrations of glucose in osteogenic medium at 4 wk of culture. At all concentrations of glucose, osteocalcin production in the NSx group was higher compared with the Ox group. In the Ox group, osteocalcin production was decreased significantly with glucose concentrations up to 8.0 mM, but increased with concentrations above 8.0 mM. In the NSx group, the trend in osteocalcin deposition associated with glucose concentrations was similar to the Ox group (Fig. 3B).

Extracellular matrix mineralization

Ca deposition was determined on the surface of both groups at the four concentrations of glucose in osteogenic medium at 4 wk of culture. At all glucose concentrations, Ca deposition in the NSx group was higher than in the Ox group. In the Ox group, Ca deposition decreased significantly with glucose concentration up to 8.0 mM, but increased with concentrations above 8.0 mM. In the NSx group, the trend in Ca deposition associated with glucose concentrations was similar to the Ox group (Fig. 4A).

ECM mineralization was assessed by Alizarin Red staining at 4 wk of osteogenic culture (Fig. 4B). The NSx group produced abundant mineralization nodules that were larger than those of the Ox group were. In addition, the mineralization deposits

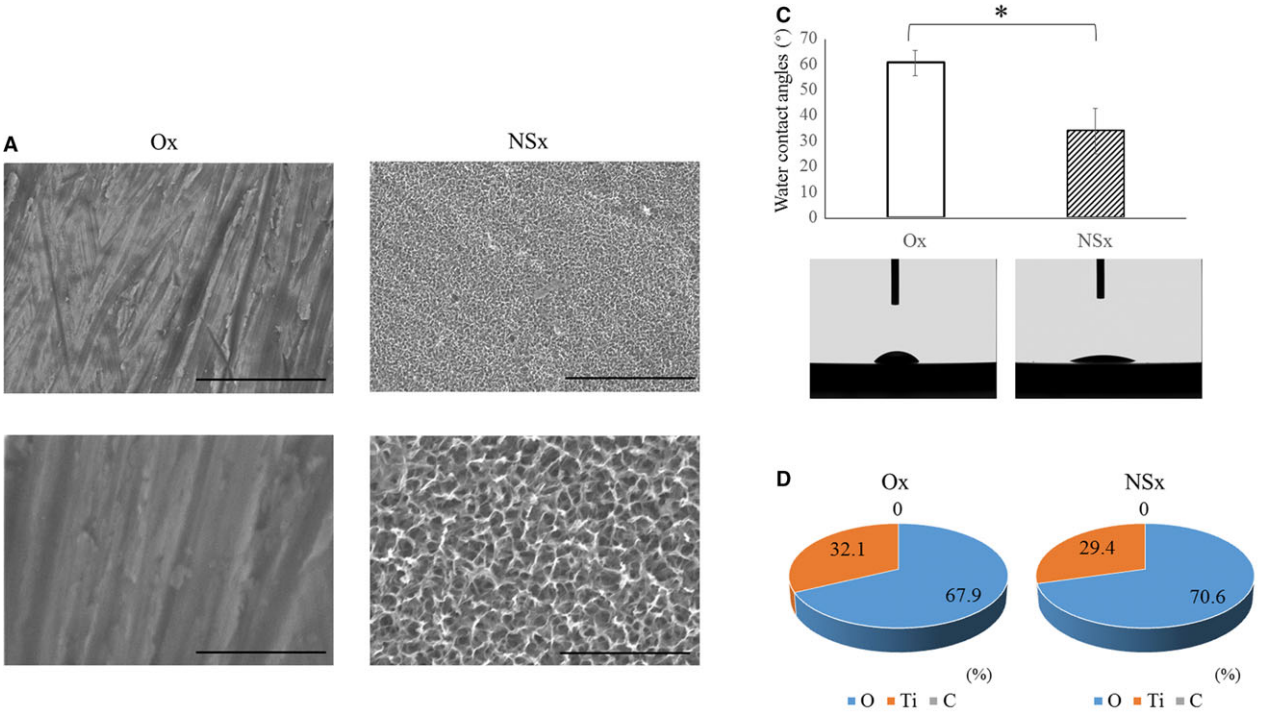

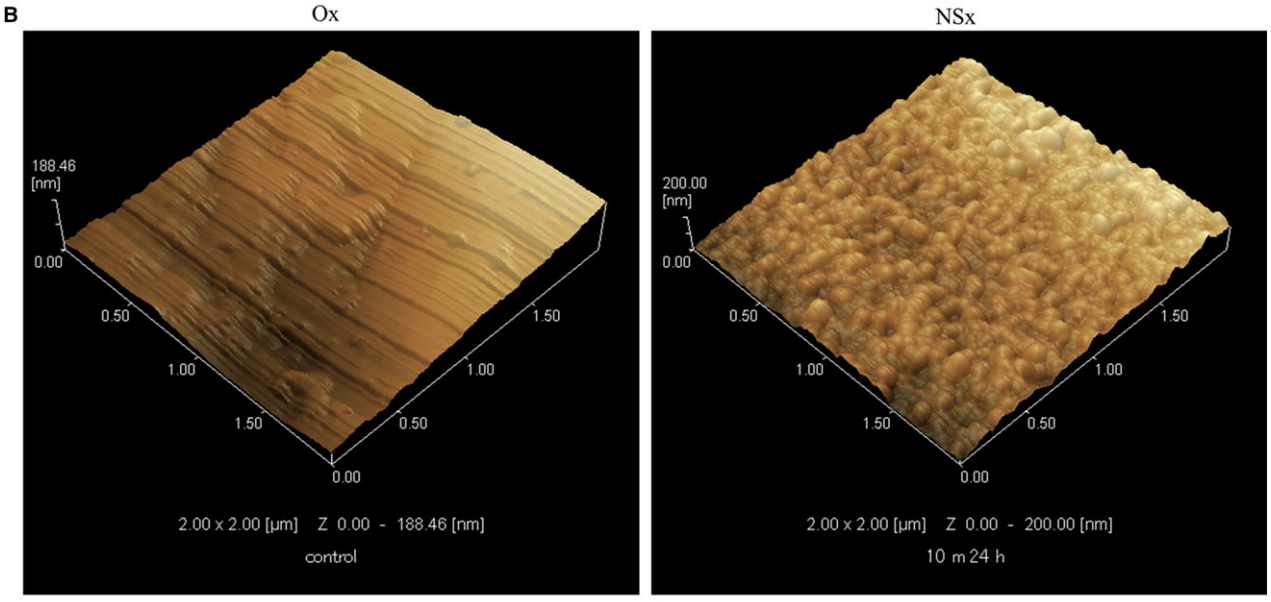

	Ox	NSx
Ra	25.5	47.939
Rz	282	511.354

(nm)

Fig. 1. Modified titanium surface analysis. (A) Titanium surface structure analyzed by scanning electron micrographs of disks from the heated titanium without nano-sheet (Ox) and heated titanium nano-sheet (NSx) groups. Upper images, at a lower magnification of ×10,000, show the overall microscale topography. Scale bars are 50 μm. Lower images, at a higher magnification of ×50,000, reveal the nanoscale texture. Scale bars are 10 μm. (B) Titanium surface roughness analyzed by atomic force microscopy of disks in the Ox and NSx groups. Images are at a higher magnification of ×50,000. Ra value is the arithmetic average roughness (nm), Rz value is the 10-point average roughness (nm). (C) Water contact angles of disks in the Ox and NSx groups. Upper graph depicts the contact angles, with the lower images observed adjacent to where the contact angles were measured. *$p < 0.05$. (D) Constituent elements of titanium surface of Ox and NSx disks. C, carbon; O, oxygen; Ti, titanium.

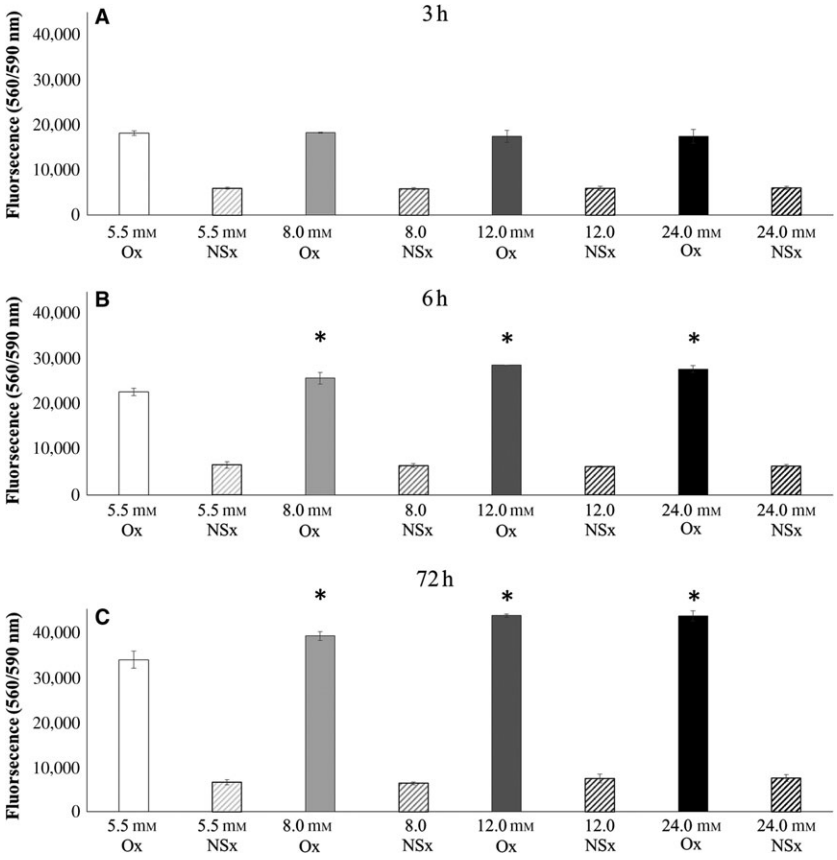

Fig. 2. Cell proliferation on disks from heated titanium without the nano-sheet (Ox) group and heated titanium with the nano-sheet (NSx) group: (A) after 3 h of incubation, (B) after 6 h of incubation; (C) after 72 h of incubation in medium with glucose at four concentrations (5.5, 8.0, 12.0 or 24.0 mM) measured by the CellTiter-Blue Cell Viability Assay. $p < 0.05$. *: vs. Ox 5.5 mM. There were no significant differences between the four glucose concentrations in the NSx group.

differed in appearance according to glucose concentration.

The Ca/P ratio was determined on the surface of both groups at the four concentrations of glucose in osteogenic medium at 4 wk of culture (Fig. 4C). At all concentrations of glucose, the Ca/P ratios in the NSx group were higher than those in the Ox group were. In the Ox group, the Ca/P ratio decreased significantly with glucose concentrations up to 8.0 mM, but increased with those above 8.0 mM. In the NSx group, the trend in Ca/P ratio associated with glucose concentrations was similar to the Ox group.

Inflammatory cytokine expression

The expression of inflammatory cytokine genes, including TNF-α, IL-1β and IL-6 was assessed by real-time PCR (Fig. 5). Gene expression levels of TNF-α (Fig. 5A), IL-1β (Fig. 5B) and IL-6 (Fig. 5C) indicated that the NSx group induced lower mRNA levels than the Ox group, except at a glucose concentration of 24 mM for 3 wk, when levels were comparable.

In the Ox groups, the gene expression of TNF-α (Fig. 5A) was increased with glucose concentrations up to 8.0 mM, but decreased with concentrations above 8.0 mM. In the NSx group, however, TNF-α gene expression was not associated with glucose concentrations, whereby low-level TNF-α gene expression was maintained. In the Ox group, the gene expression of IL-1β (Fig. 5B) was increased with glucose concentrations up to 8.0 mM, but decreased with concentrations above 8.0 mM at 3 wk. However, levels were maintained higher at glucose concentrations over 8.0 mM at 4 wk. In the NSx group, low-level gene expression of IL-1β was maintained regardless of glucose concentration. In the Ox group, IL-6 gene expression (Fig. 5C) was higher in high glucose concentrations at 3 wk, but in the NSx group, IL-6 expression was comparable to that at 5.5 mM glucose concentration.

Discussion

To the best of our knowledge, the present study is the first to investigate the effects of high glucose concentrations on titanium surfaces with a nano-network structure on osteogenesis and mineralization quality. Although high glucose concentrations reduced ALP activity, osteocalcin production and Ca deposition, all of these were induced on the titanium surface with or without the nanostructure.

Delayed bone healing around implant fixtures and insufficient osseointegration are apparent in patients with DM (6–12). Gerritsen *et al.* (15) reported that peri-implantitis was further developed in patients with DM than in those without; however, if osseointegration is acquired during early-stage healing in patients with DM, the level of osseointegration is similar to those without DM (34). Therefore, we isolated BM-MSCs from type II DM rats in this study. The surface of the implant fixture is first colonized by BM-MSCs disturbed by drilling for placement of the implant. This colonization is an important step in osseointegration. Ohgushi *et al.* (35) reported that the calcified substrate formed extracellularly of BM-MSCs was morphologically similar to the osseous tissue of the living body. Our previous study confirmed that hard tissue formed by BM-MSCs on titanium surfaces with nano-network structures (33).

Many different surface treatments for dental implant have been developed, including chemical, electrical and photodynamic (16–20,36). In this study, we focused on the chemical

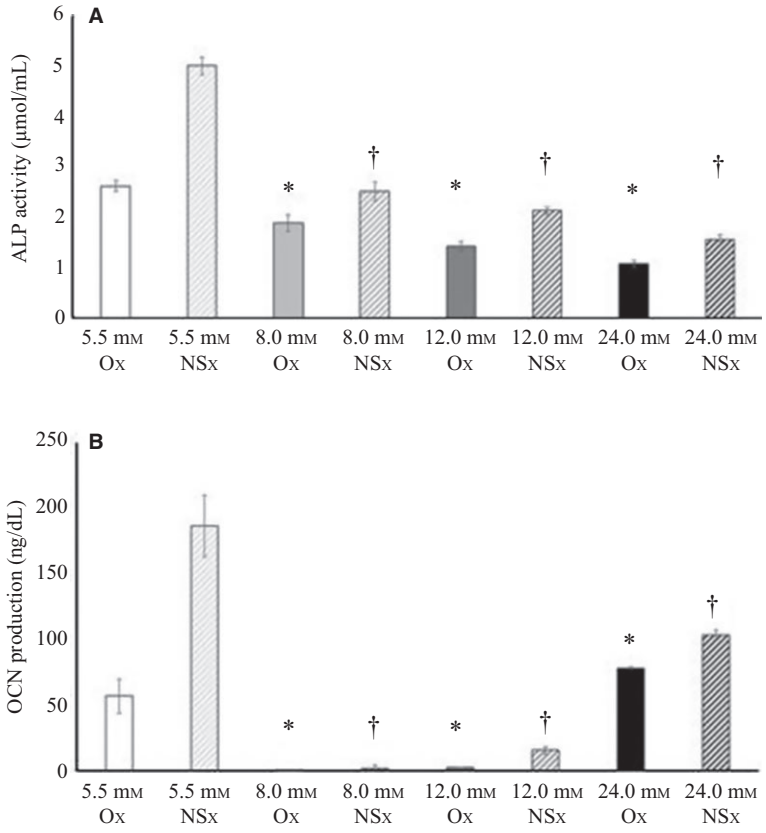

Fig. 3. Effect of glucose concentration on ALP activity and OCN production. (A) ALP activity of bone marrow-derived mesenchymal stromal cells on disks from the heated titanium without nano-sheet (Ox) and heated titanium nano-sheet (NSx) groups after 1 wk of culture in osteogenic medium with four glucose concentrations (5.5, 8.0, 12.0 or 24.0 mM). $p < 0.05$. *: vs. Ox 5.5 mM. †: vs. NSx 5.5 mM. (B) OCN production by bone marrow-derived mesenchymal stromal cells seeded on disks from Ox and NSx groups after 4 wk of culture in osteogenic medium with four glucose concentrations (5.5, 8.0, 12.0 or 24.0 mM). $p < 0.05$. *: vs. Ox 5.5 mM, †: vs. NSx 5.5 mM. ALP, alkaline phosphatase; OCN, osteocalcin.

treatment of dental implants. We have previously reported that pure titanium disks immersed in 10 M NaOH solution for 24 h form a nano-structure on the titanium surface (27). The nano-structure produced provides increased wettability, enhanced hard tissue differentiation and anti-inflammation.

Wettability is important during the first stage of implant healing, just after implant fixture placement (37). Immediately following implantation, the implant is surrounded by blood, including BM-MSCs from the bone surrounding the implant fixture. Indeed, our results have indicated that in the NSx group, hard tissue differentiation and anti-inflammation were induced to a greater extent.

Additionally, a passivation layer of titanium oxide (TiO_2) forms naturally on the surface of titanium disks. The oxygen content is higher in the NSx disks than in the Ox disks, because of the larger surface area offered by the nano-structure on the titanium surface of NSx disks. By changing the properties of the oxide layer, different tissue responses can be induced. Heat treatment increases the levels of oxygen and removes carbon, thus creating an oxide layer and removing impurities on the titanium surface. First, heat treatment of the sample likely induces crystallization and anatase formation or further promotes rutile formation from available TiO_2, resulting in potential enhancement of photocatalytic properties along the gradient (38). Second, the carbon ratio on the titanium surface increases with the passage of time. Moreover, it reduces the wettability of the titanium surface, and inhibits the proliferation of osteoblasts, ALP activity and calcification (18–20,39,40).

The structure of the titanium surface does not greatly influence the proliferation, extension or sequence of cells, as it is differentiation that plays the most important role.

The Ox disks promote more cell proliferation than the NSx disks. In other words, the Ox disks grow oral bacteria more easily than the NSx disks. Moreover, surface roughness plays an important role in the differentiation of cells. Martin *et al.* (41) reported that there is more calcification and collagen for osteoblasts to attach to on a rough surface than on a smooth surface. The production of prostaglandin E_2 and transforming growth factor-β increased significantly and the response of osteoblast-like cells for 1α,25-dihydroxyvitamin D_3 increased, significantly increasing the production of osteocalcin and increasing ALP activity in particular (42,43). Similarly, ALP activity and osteocalcin production on the NSx disks were higher than those on the Ox disks in this study. Thus, treatment of titanium surfaces by immersion in 10 M NaOH solution at room temperature for 24 h and heating at 600°C for 1 h formed nano-structures of TiO_2 on the titanium surface, which is suggested to improve cell differentiation of BM-MSCs. ALP is associated with bone formation and calcification and its activity is regarded as a relatively early marker of osteoblast growth (44). Lack of insulin activity reduces osteoblastic function, and a high glucose environment inhibits intracellular signal transduction in osteoblast cells (45,46). High glucose concentration inhibits BM-MSC function and ALP activity on titanium surfaces, thereby inhibiting bone formation. Nano-scale modification of the titanium surface promoted ALP activity, but this was affected by glucose concentration.

Osteocalcin plays a vital role in the regulation of glucose metabolism (47–

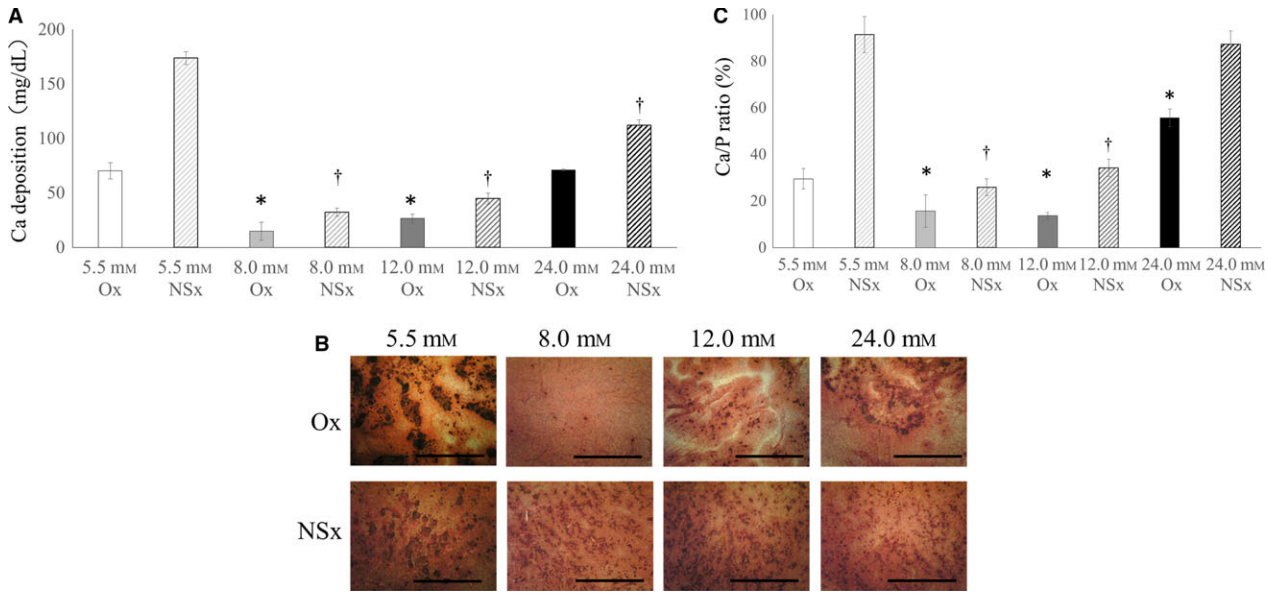

Fig. 4. Effect of glucose concentrations on mineralization. (A) Ca deposition by bone marrow-derived mesenchymal stromal cells seeded on disks from heated titanium without nano-sheet (Ox) and heated titanium nano-sheet (NSx) groups after 4 wk of culture in osteogenic medium with four glucose concentrations (5.5, 8.0, 12.0 or 24.0 mM). $p < 0.05$. *: vs. Ox 5.5 mM, †: vs. NSx 5.5 mM. (B) Ca deposition is stained by Alizarin Red. Scale bars are 1 mm. (C) Ca/P ratio of bone marrow-derived mesenchymal stromal cells seeded on disks from Ox and NSx groups after 4 wk of culture in osteogenic medium of four glucose concentrations (5.5, 8.0, 12.0 or 24.0 mM). $p < 0.05$. *: vs. Ox 5.5 mM, †: vs. NSx 5.5 mM.

49). Typically, if bone metabolism is reduced, then osteocalcin production is also inhibited; however, in this study osteocalcin deposition increased at glucose concentrations above 8.0 mM. Lee *et al.* (50) revealed that osteocalcin acts as a hormone that regulates glucose metabolism and fat mass, showing that osteocalcin-knockout mice displayed decreased β-cell proliferation, glucose intolerance and insulin resistance. In the Kanazawa *et al.* (51) study, serum osteocalcin levels were significantly and negatively correlated with glycemic control in both men and postmenopausal women with type II DM, in line with the findings of the current investigation. According to Okazaki *et al.* (52), improvement of poorly controlled glycemic status in type II DM helps modulate bone turnover, reducing markers for bone resorption and increasing osteocalcin. BM-MSCs produced more osteocalcin following stimulation with higher levels of glucose. We consider that the role of osteocalcin in promoting bone metabolism and the secretion of insulin is significantly different at glucose concentrations of 8.0 mM. A concentration of 8.0 mM glucose is usually observed in a patient with well-controlled DM and after a meal in non-DM patients, while concentrations of 12.0 and 24.0 mM are observed in severe DM. It is not necessary for insulin that osteocalcin is secreted at usually high glucose concentration (8.0 mM). It is necessary for insulin that osteocalcin is secreted at severe high glucose concentration (12.0 and 24.0 mM). Further, high glucose concentrations interrupt cell communication related to bone metabolism, as osteocalcin secretion was lower at 8.0 mM than at 5.5 mM. Therefore, osteocalcin secretion at 8.0 mM was lower than at other glucose concentrations. Osteocalcin is non-collagenous protein of bone that plays a role in Ca deposition.

According to osteocalcin production, Ca deposition increased at glucose concentrations above 8.0 mM; however, Ca deposition at high glucose concentration was not the same quality as that at normal glucose concentration. Balint *et al.* (53) showed that in the presence of elevated glucose concentration, osteoblast proliferation is enhanced, while *in vitro* bone formation is significantly inhibited. Therefore, we examined the Ca/P ratio of hard tissue created on the titanium surface. Kourkoumelis *et al.* (54) showed that bone quality, in addition to bone density, plays an important role in bone strength and is strongly related to the Ca/P ratio. Therefore, it might be possible to use this biomarker for the effective diagnostic and classification criteria of osteoporosis and related diseases. In this study, P deposition decreased at high glucose concentration and this phenomenon was associated with ALP activity. ALP is a glycoprotein that is present on cell membranes, which degrades inorganic phosphorus and alcohol to form phosphoric acid ester under alkaline conditions (pH 9–11). Indeed, high glucose concentration reduced ALP activity and P deposition and induced the Ca/P ratio, so the balance between Ca and P collapsed. We suggested that high glucose concentration increased the volume of hard tissue formation, but the quality of hard tissue was poor. Furthermore, mineralization quality was dependent on glucose concentration, even with the nano-scale modified titanium surface.

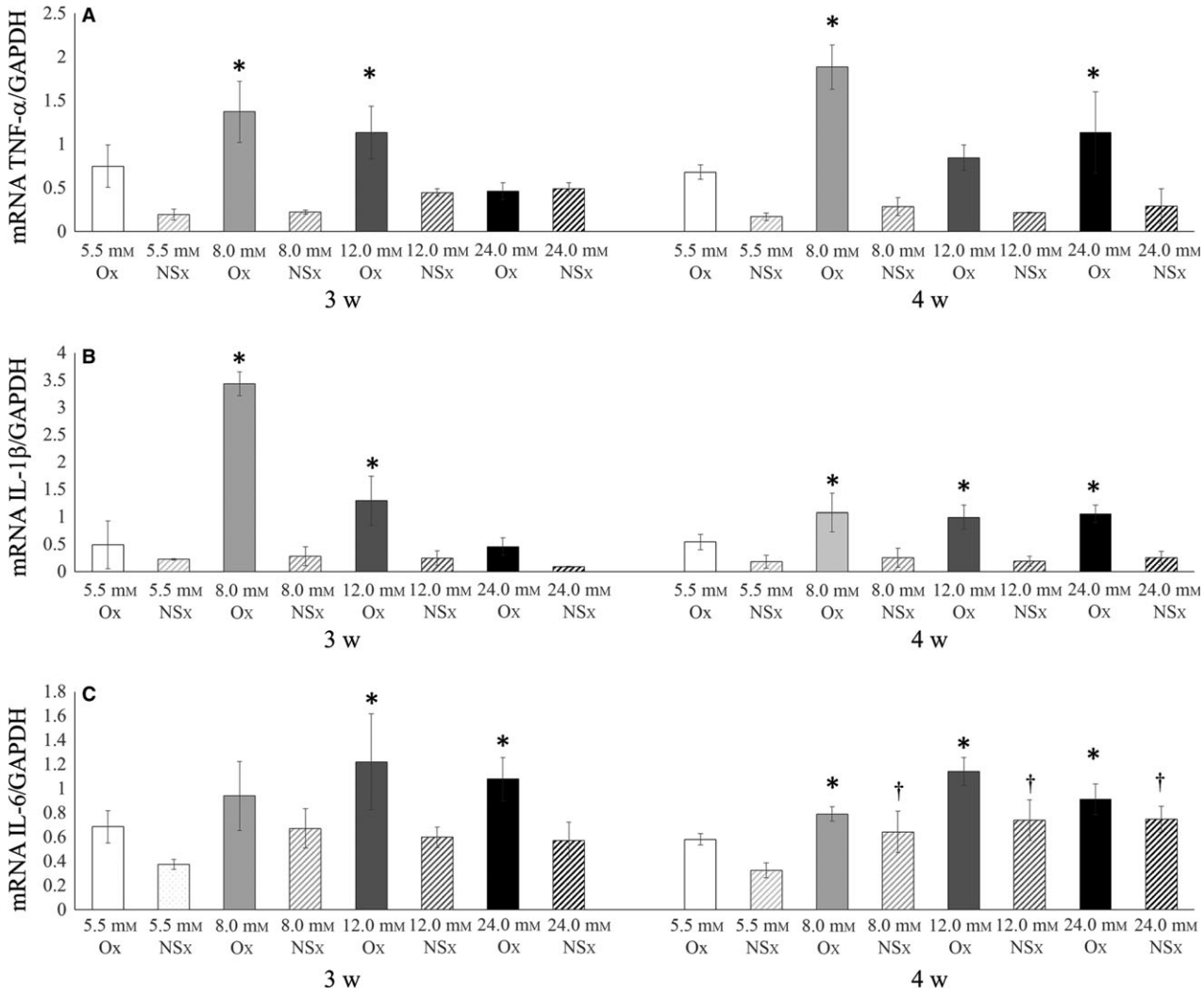

Fig. 5. Inflammatory cytokine gene expression by bone marrow-derived mesenchymal stromal cells cultured on disks from heated titanium without nano-sheet (Ox) and heated titanium nano-sheet (NSx) groups after 3 and 4 wk of culture in osteogenic medium with four glucose concentrations (5.5, 8.0, 12.0 or 24.0 mM). TNF-α (A), IL-1β (B), IL-6 (C). Data were obtained from real-time polymerase chain reaction analysis and are shown as means ± SD expressed relative to GAPDH. $p < 0.05$. *: vs. Ox 5.5 mM, †: vs. NSx 5.5 mM. IL, interleukin; TNF, tumor necrosis factor.

Inflammation is thought to be closely related to bone metabolism (55). TNF-α, IL-1β and IL-6 play important roles in the inflammatory response, but their exact role in osteogenic differentiation is controversial (56,57). We isolated primary BM-MSCs from GK rats in this study. The GK rat is a model of type II DM – plasma insulin is increased at the time of satiation and mild insulin resistance is increased (58,59). Additionally, TNF-α inhibits the uptake of intracellular glucose, leading to hyperglycemia. We suggest that TNF-α expression decreased at abnormally high glucose concentrations (12.0 and 24.0 mM) and increased at 8.0 mM.

Therefore, the high glucose concentration increased the inflammatory cytokine expression of the cells stress by high glucose concentration, but the nano-modified process decreased this expression. We demonstrated that the titanium surface type modified with 10 M NaOH to create a nano-network structure promoted hard tissue formation and could be an effective method of improving titanium's biological properties (27). Additionally, ALP activity, osteocalcin production, Ca deposition and Ca/P ratio on the modified surface were higher than those on the smooth surface were. The layer of oxidation on the pure titanium surface combined with the sodium ions in sodium hydroxide to form a titanate structure, which plays a role in osteogenesis (60).

Consequently, this improved biocompatibility enhanced the suppression of inflammatory cytokines, better enabling hard tissue formation around the titanium surface for osseointegration, even in the presence of high glucose concentration. In summary, the high glucose concentration likely demotes osteogenesis in at

least two ways: by demoting cell osteogenic differentiation and promoting the diabetic inflammatory response.

Although most authors do not propose DM as a contraindication or a significant risk factor for dental implant therapy, some studies suggest that there is a reduced success rate in surgical procedures associated with dental implant therapy in these patients. The success rate of dental implants in patients with DM varies between 68% and 100% (8,28,61–64). Additionally, dental implant success rate has been shown to have lower long-term maintenance, even if the success rate is initially high in patients with DM (65). In patients with DM and good glycemic control, the reported success rate of dental implants differs greatly among studies, because glucose concentration levels and the type of titanium surface treatment used also differ.

We suggest that the Ca/P ratio is an important inspection standard for the evaluation of hard tissue formation and differences in quality associated with different glucose concentrations and implant surface treatments.

Conclusion

Glucose concentration affected the volume and quality of mineralized hard tissue formation on the surface of titanium implants with or without nano-scale structure. We suggest that by maintaining a normal glucose concentration during the initial osseointegration period, this could increase the success rate of dental implantation in patients with DM.

Acknowledgements

The author would like to thank Prof. Toru Sekino from Osaka University for making the "Nano sheet" and for helpful suggestions. This work was supported by a Grant-in-Aid for Scientific Research (26861664, 15H06742, 16K11617, 16K20524) from the Japan Society for the Promotion of Science, and a Research Promotion Grant (16-04) from Osaka Dental University.

Conflict of interest

The authors declare that they have no conflicts of interest.

References

1. King GL. The role of inflammatory cytokines in diabetes and its complications. *J Periodontol* 2008;**79**:1527–1534.
2. American Diabetes Association. Diagnosis and classification of diabetes mellitus [Editorial]. *Diabetes Care* 2005;**28**:37–42.
3. Ebersole JL, Holt SC, Hansard R, Novak MJ. Microbiologic and immunologic characteristics of periodontal disease in Hispanic Americans with type 2 diabetes. *J Periodontol* 2008;**79**:637–646.
4. Lalla E, Lamster IB, Drury S, Fu C, Schmidt AM. Hyperglycemia, glycoxidation and receptor for advanced glycation endproducts: potential mechanisms underlying diabetic complications, including diabetes-associated periodontitis. *Periodontol 2000* 2000;**23**:50–62.
5. Katyayan PA, Katyayan M, Shah RJ. Rehabilitative considerations for dental implants in the diabetic patient. *J Indian Prosthodont Soc* 2013;**13**:175–183.
6. Retzepi M, Donos N. The effect of diabetes mellitus on osseous healing. *Clin Oral Implants Res* 2010;**21**:673–681.
7. von Wilmowsky C, Stockmann P, Harsch I *et al*. Diabetes mellitus negatively affects peri-implant bone formation in the diabetic domestic pig. *J Clin Periodontol* 2011;**38**:771–779.
8. Moy PK, Medina D, Shetty V, Aghaloo TL. Dental implant failure rates and associated risk factors. *Int J Oral Maxillofac Implants* 2005;**20**:569–577.
9. Oates TW, Dowell S, Robinson M, McMahan CA. Glycemic control and implant stabilization in type 2 diabetes mellitus. *J Dent Res* 2009;**88**:367–371.
10. Javed F, Romanos GE. Impact of diabetes mellitus and glycemic control on the osseointegration of dental implants: a systematic literature review. *J Periodontol* 2009;**80**:1719–1730.
11. de Molon RS, Morais-Camilo JA, Verzola MH, Faeda RS, Pepato MT, Marcantonio E Jr. Impact of diabetes mellitus and metabolic control on bone healing around osseointegrated implants: removal torque and histomorphometric analysis in rats. *Clin Oral Implants Res* 2013;**24**:831–837.
12. Kotsovilis S, Karoussis IK, Fourmousis I. A comprehensive and critical review of dental implant placement in diabetic animals and patients. *Clin Oral Implants Res* 2006;**17**:587–599.
13. Drago L, Bortolin M, De ecchi E *et al*. Antibiofilm activity of sandblasted and laser-modified titanium against microorganisms isolated from peri-implantitis lesions. *J Chemother* 2016;**30**:1–7.
14. Rios FG, Viana ER, Ribeiro GM, González JC, Abelenda A, Peruzzo DC. Temperature evaluation of dental implant surface irradiated with high-power diode laser. *Lasers Med Sci* 2016;**30**:1–8.
15. Gerritsen M, Lutterman JA, Jansen JA. Wound healing around bone-anchored percutaneous devices in experimental diabetes mellitus. *J Biomed Mater Res* 2000;**53**:702–709.
16. Sykaras N, Iacopino AM, Marker VA, Triplett RG, Woody RD. Implant materials, designs, and surface topographies: their effect on osseointegration. A literature review. *Int J Oral Maxillofac Implants* 2000;**15**:675–690.
17. Le Guéhennec L, Soueidan A, Layrolle P, Amouriq Y. Surface treatments of titanium dental implants for rapid osseointegration. *Dent Mater* 2007;**23**:844–854.
18. Att W, Hori N, Iwasa F, Yamada M, Ueno T, Ogawa T. The effect of UV-photofunctionalization on the time-related bioactivity of titanium and chromium-cobalt alloys. *Biomaterials* 2009;**30**:4268–4276.
19. Suzuki T, Hori N, Att W *et al*. Ultraviolet treatment overcomes time-related degrading bioactivity of titanium. *Tissue Eng Part A* 2009;**15**:3679–3688.
20. Hori N, Ueno T, Suzuki T *et al*. Ultraviolet light treatment for the restoration of age-related degradation of titanium bioactivity. *Int J Oral Maxillofac Implants* 2010;**25**:49–62.
21. Albrektsson T, Albrektsson B. Osseointegration of bone implants. A review of an alternative mode of fixation. *Acta Orthop Scand* 1987;**58**:567–577.
22. Davies JE. Understanding peri-implant endosseous healing. *J Dent Educ* 2003;**67**:932–949.
23. Albrektsson T, Wennerberg A. Oral implant surfaces: Part 1 – review focusing on topographic and chemical properties of different surfaces and *in vivo* responses to them. *Int J Prosthodont* 2004;**17**:536–543.
24. Gotfredsen K, Nimb L, Hjörting-Hansen E, Jensen JS, Holmén A. Histomorphometric and removal torque analysis for TiO_2-blasted titanium implants. An experimental study on dogs. *Clin Oral Implants Res* 1992;**3**:77–84.
25. Lossdörfer S, Schwartz Z, Wang L *et al*. Microrough implant surface topographies increase osteogenesis by reducing osteoclast formation and activity. *J Biomed Mater Res A* 2004;**70**:361–369.
26. Brunski JB, Puleo DA, Nanci A. Biomaterials and biomechanics of oral and

maxillofacial implants: current status and future developments. *Int J Oral Maxillofac Implants* 2000;**15**:15–46.
27. Komasa S, Taguchi Y, Nishida H, Tanaka M, Kawazoe T. Bioactivity of nanostructure on titanium surface modified by chemical processing at room temperature. *J Prosthodont Res* 2012;**56**:170–177.
28. Khandelwal N, Oates TW, Vargas A, Alexander PP, Schoolfield JD, Alex McMahan C. Conventional SLA and chemically modified SLA implants in patients with poorly controlled type 2 diabetes mellitus – a randomized controlled trial. *Clin Oral Implants Res* 2013;**24**:13–19.
29. McCracken MS, Aponte-Wesson R, Chavali R, Lemons JE. Bone associated with implants in diabetic and insulin-treated rats. *Clin Oral Implants Res* 2016;**17**:495–500.
30. Chen NK, Tan SY, Udolph G, Kon OL. Insulin expressed from endogenously active glucose-responsive EGR1 promoter in bone marrow mesenchymal stromal cells as diabetes therapy. *Gene Ther* 2010;**17**:592–605.
31. Jung EJ, Kim SC, Wee YM *et al*. Bone marrow-derived mesenchymal stromal cells support rat pancreatic islet survival and insulin secretory function *in vitro*. *Cytotherapy* 2011;**13**:19–29.
32. Yan T, Venkat P, Chopp M *et al*. Neurorestorative responses to delayed human mesenchymal Stromal cells treatment of stroke in type 2 diabetic rats. *Stroke* 2016;**47**:2850–2858.
33. Xing H, Komasa S, Taguchi Y, Sekino T, Okazaki J. Osteogenic activity of titanium surfaces with nanonetwork structures. *Int J Nanomedicine* 2014;**9**:1741–1755.
34. Colombo JS, Balani D, Sloan AJ, Crean SJ, Okazaki J, Waddington RJ. Delayed osteoblast differentiation and altered inflammatory response around implants placed in incisor sockets of type 2 diabetic rats. *Clin Oral Implants Res* 2011;**22**:578–586.
35. Ohgushi H, Dohi Y, Katuda T, Tamai S, Tabata S, Suwa Y. *In vitro* bone formation by rat marrow cell culture. *J Biomed Mater Res* 1996;**32**:333–340.
36. Ikeda T, Hagiwara Y, Hirota M *et al*. Effect of photofunctionalization on fluoride-treated nanofeatured titanium. *J Biomater Appl* 2014;**28**:1200–1212.
37. Ogawa T. Ultraviolet photofunctionalization of titanium implants. *Int J Oral Maxillofac Implants* 2014;**29**:95–102.
38. Unosson E, Welch K, Persson C, Engqvist H. Stability and prospect of UV/H_2O_2 activated titania films for biomedical use. *Appl Surf Sci* 2013;**285**:317–323.
39. Hori N, Att W, Ueno T *et al*. Age-dependent degradation of the protein adsorption capacity of titanium. *J Dent Res* 2009;**88**:663–667.
40. Att W, Hori N, Takeuchi M *et al*. Time-dependent degradation of titanium osteoconductivity: an implication of biological aging of implant materials. *Biomaterials* 2009;**30**:5352–5363.
41. Martin JY, Schwartz Z, Hummert TW *et al*. Effect of titanium surface roughness on proliferation, differentiation, and protein synthesis of human osteoblast-like cells (MG63). *J Biomed Mater Res* 1995;**29**:389–401.
42. Kieswetter K, Schwartz Z, Hummert TW *et al*. Surface roughness modulates the local production of growth factors and cytokines by osteoblast-like MG-63 cells. *J Biomed Mater Res* 1996;**32**:55–63.
43. Boyan BD, Batzer R, Kieswetter K *et al*. Titanium surface roughness alters responsiveness of MG63 osteoblast-like cells to 1 alpha,25-$(OH)_2D_3$. *J Biomed Mater Res* 1998;**39**:77–85.
44. Wlodarski KH, Reddi AH. Alkaline phosphatase as a marker of osteoinductive cells. *Calcif Tissue Int* 1986;**39**:382–385.
45. Terada M, Inaba M, Yano Y, Hasuma T, Nishizawa Y, Morii H. Growth-inhibitory effect of a high glucose concentration on osteoblast-like cells. *Bone* 1998;**22**:17–23.
46. Williams B, Schrier RW. Characterization of glucose-induced *in situ* protein kinase C activity in cultured vascular smooth muscle cells. *Diabetes* 1992;**41**:1464–1472.
47. Ferron M, Hinoi E, Karsenty G, Ducy P. Osteocalcin differentially regulates beta cell and adipocyte gene expression and affects the development of metabolic diseases in wild-type mice. *Proc Natl Acad Sci U S A* 2008;**105**:5266–5270.
48. Motyl KJ, McCabe LR, Schwartz AV. Bone and glucose metabolism: a two-way street. *Arch Biochem Biophys* 2010;**503**:2–10.
49. Wang Q, Zhang B, Xu Y, Xu H, Zhang N. The Relationship between Serum Osteocalcin Concentration and Glucose Metabolism in Patients with Type 2 Diabetes Mellitus. *Int J Endocrinol* 2013;**2013**:1–7.
50. Lee NK, Sowa H, Hinoi E *et al*. Endocrine regulation of energy metabolism by the skeleton. *Cell* 2007;**130**:456–469.
51. Kanazawa I, Yamaguchi T, Yamamoto M *et al*. Serum osteocalcin level is associated with glucose metabolism and atherosclerosis parameters in type 2 diabetes mellitus. *J Clin Endocrinol Metab* 2009;**94**:45–49.
52. Okazaki R, Totsuka Y, Hamano K *et al*. Metabolic improvement of poorly controlled noninsulin-dependent diabetes mellitus decreases bone turnover. *J Clin Endocrinol Metab* 1997;**82**:2915–2920.
53. Balint E, Szabo P, Marshall CF, Sprague SM. Glucose-induced inhibition of *in vitro* bone mineralization. *Bone* 2001;**28**:21–28.
54. Kourkoumelis N, Balatsoukas I, Tzaphlidou M. Ca/P concentration ratio at different sites of normal and osteoporotic rabbit bones evaluated by Auger and energy dispersive X-ray spectroscopy. *J Biol Phys* 2012;**38**:279–291.
55. Okabe T, Matsushima K. Regulation of ALP activity by TNF-alpha on human dental pulp. *J Endod* 2006;**32**:516–520.
56. Wang Q, Li H, Xiao Y *et al*. Locally controlled delivery of TNFα antibody from a novel glucose-sensitive scaffold enhances alveolar bone healing in diabetic conditions. *J Control Release* 2015;**206**:232–242.
57. El-Azab MF, Attia FM, El-Mowafy AM. Novel role of curcumin combined with bone marrow transplantation in reversing experimental diabetes: effects on pancreatic islet regeneration, oxidative stress, and inflammatory cytokines. *Eur J Pharmacol* 2011;**658**:41–48.
58. Berthelier C, Kergoat M, Portha B. Lack of deterioration of insulin action with aging in the GK rat: a contrasted adaptation as compared with nondiabetic rats. *Metabolism* 1997;**46**:890–896.
59. Bisbis S, Bailbe D, Tormo MA *et al*. Insulin resistance in the GK rat: decreased receptor number but normal kinase activity in liver. *Am J Physiol* 1993;**265**:E807–E813.
60. Kasuga T, Hiramatsu M, Hoson A, Sekino T, Niihara K. Formation of titanium oxide nanotube. *Langmuir* 1998;**14**:3160–3163.
61. Balshi TJ, Wolfinger GJ. Dental implants in the diabetic patient: a retrospective study. *Implant Dent* 1999;**8**:355–359.
62. Fiorellini JP, Nevins ML. Dental implant considerations in the diabetic patient. *Periodontol 2000* 2000;**23**:73–77.
63. Farzad P, Andersson L, Nyberg J. Dental implant treatment in diabetic patients. *Implant Dent* 2002;**11**:262–267.
64. Peled M, Ardekian L, Tagger-Green N, Gutmacher Z, Machtei EE. Dental implants in patients with type 2 diabetes mellitus: a clinical study. *Implant Dent* 2003;**12**:16–22.
65. Dowell S, Oates TW, Robinson M. Implant success in people with type 2 diabetes mellitus with varying glycemic control: a pilot study. *J Am Dent Assoc* 2007;**138**:355–361.